Published in final edited form as:
Mol Imaging Biol. 2012 February ; 14(1): 88–95. doi:10.1007/s11307-011-0477-3.

First Experience with Clinical-Grade [^{18}F]FPP (RGD)$_2$: An Automated Multi-step Radiosynthesis for Clinical PET Studies

Frederick T. Chin[1], **Bin Shen**[1], **Shuanglong Liu**[1], **Rhona A. Berganos**[1], **Edwin Chang**[1], **Erik Mittra**[2], **Xiaoyuan Chen**[3], and **Sanjiv S. Gambhir**[1,2]

[1]Molecular Imaging Program at Stanford (MIPS), Departments of Radiology and Bioengineering, Bio-X Program, Stanford University School of Medicine, Stanford, CA 94305, USA

[2]Department of Radiology, Division of Nuclear Medicine, Molecular Imaging Program, Stanford, CA 94305, USA

[3]Laboratory for Molecular Imaging and Nanomedicine, National Institute of Biomedical Imaging and Bioengineering, National Institutes of Health, Bethesda, MD 20892, USA

Abstract

Purpose—A reliable and routine process to introduce a new ^{18}F-labeled dimeric RGD-peptide tracer ([^{18}F]FPP(RGD)$_2$) for noninvasive imaging of $\alpha_v\beta_3$ expression in tumors needed to be developed so the tracer could be evaluated for the first time in man. Clinical-grade [^{18}F]FPP (RGD)$_2$ was screened in mouse prior to our first pilot study in human.

Procedures—[^{18}F]FPP(RGD)$_2$ was synthesized by coupling 4-nitrophenyl-2-[^{18}F]fluoropropionate ([^{18}F]NPE) with the dimeric RGD-peptide (PEG$_3$-c(RGDyK)$_2$). Imaging studies with [^{18}F]FPP (RGD)$_2$ in normal mice and a healthy human volunteer were carried out using small animal and clinical PET scanners, respectively.

Results—Through optimization of each radiosynthetic step, [^{18}F]FPP(RGD)$_2$ was obtained with RCYs of 16.9±2.7% (*n*=8, EOB) and specific radioactivity of 114±72 GBq/μmol (3.08±1.95 Ci/μmol; *n*=8, EOB) after 170 min of radiosynthesis. In our mouse studies, high radioactivity uptake was only observed in the kidneys and bladder with the clinical-grade tracer. Favorable [^{18}F]FPP (RGD)$_2$ biodistribution in human studies, with low background signal in the head, neck, and thorax, showed the potential applications of this RGD-peptide tracer for detecting and monitoring tumor growth and metastasis.

Conclusions—A reliable, routine, and automated radiosynthesis of clinical-grade [^{18}F]FPP(RGD)$_2$ was established. PET imaging in a healthy human volunteer illustrates that [^{18}F]FPP(RGD)$_2$ possesses desirable pharmacokinetic properties for clinical noninvasive imaging of $\alpha_v\beta_3$ expression. Further imaging studies using [^{18}F]FPP(RGD)$_2$ in patient volunteers are now under active investigation.

Keywords

Oncology; Peptides; Radiopharmaceuticals; [^{18}F]FPP(RGD)$_2$; Automated radiosynthesis; Clinical PET; Tumor angiogenesis; Integrins

Correspondence to: Frederick T. Chin; chinf@stanford.edu.

Bin Shen and Shuanglong Liu contributed equally to this work.

Conflicts of Interest. The authors declare that they have no conflicts of interest.

Introduction

Angiogenesis is the process in which new capillaries are formed by outgrowth from existing microvessels. This biological event is required not only for tumor growth and metastasis but is also necessary for the natural healing process after ischemic injury [1]. The $\alpha_v\beta_3$ integrin is a well-known protein target chosen for designing diagnostic and therapeutic agents aimed at tumor angiogenesis because it is highly expressed only in activated endothelial cells (ECs) of tumor neovasculature and not on normal cells or quiescent ECs [2]. Radiolabeled RGD (Arg-Gly-Asp) peptides and analogs have been specifically pursued for visualizing and quantifying $\alpha_v\beta_3$ integrin expression noninvasively in tumors with positron emission tomography (PET) [3–5]. Fluorine-18 is a popular radioisotope for labeling small molecules and peptides because of its well-suited physical half-life (109.7 min) for routine clinical use. Therefore, a number of ^{18}F-labeled RGD-peptides including [^{18}F]-galacto-RGD [6] and [^{18}F]-AH111585 [7] has been developed for PET imaging of $\alpha_v\beta_3$ integrin in the last few years. Both of these radiotracers, based on monomeric cyclic RGD-peptides, are under clinical investigation in cancer patients [8, 9]. Although the ^{18}F-labeled RGD monomer analogs can specifically bind to integrin $\alpha_v\beta_3$ expressed on the surface of some cancer cells, they have been somewhat limited due to the relatively low receptor-binding affinity and consequently low tumor uptake. In order to enhance the efficiency of tumor targeting and to obtain better *in vivo* imaging properties, the polyvalency effect was applied to develop multimeric RGD peptides. In our earlier studies with these multimeric peptides, we demonstrated that the receptor-binding affinity and tumor uptake of RGD peptides followed the order of octamer > tetramer > dimer > monomer [10–13]. The tetrameric and octameric RGD peptides possess higher receptor-binding affinity and higher tumor uptake than their dimeric and monomeric counterparts; however, the consequential higher background signals from tetrameric and octameric RGD peptides especially in the kidneys gave way to choose the more favorable dimeric scaffold for the RGD peptide. In addition, the insertion of the glycine-glycine-glycine (Gly_3) or 15-amino-4,7,10,13-tetraoxapentadecanoic acid (PEG_4) spacers was found to significantly increase the distance between the two cyclic RGD peptide motifs that resulted in an improvement in the *in vitro* receptor-binding affinity [14]. Therefore, a new ^{18}F-RGD-peptide imaging probe ([^{18}F]FPP$(RGD)_2$) was designed by conjugating ^{18}F-4-nitrophenyl-2-fluoropropionate ([^{18}F]NPE) with RGD dimeric peptide (PEG_3-c$(RGDyK)_2$ or P$(RGD)_2$, Fig. 1) that yielded our first promising results in murine models [15]. Based on these preclinical findings, our aims for this study were to present a reliable, routine and automated radiosynthesis of a new clinical-grade ^{18}F-RGD-peptide tracer ([^{18}F]FPP$(RGD)_2$) and further evaluate this higher purity tracer in both mice and human.

Material and Methods

All chemicals obtained commercially were of analytical grade (Sigma-Aldrich, USA) and used without further purification. H-11-amino-3,6,9-trioxaundecanoic acid (AEEEA)-Glu[cyclo(Arg-Gly-Asp-D-Tyr-Lys)]$_2$ (PEG_3-c$(RGDyK)_2$) (AEEEA, 99%), was purchased from Peptides International (USA). The cold reference compound, [^{19}F]FPP$(RGD)_2$, was synthesized according to our procedure previously reported [15].

No-carrier-added [^{18}F]fluoride ion was prepared on a PETtrace cyclotron (GE Medical Systems, Sweden) via the ^{18}O(p,n)^{18}F nuclear reaction by irradiating ^{18}O-enriched water (1.6 mL, >95% isotopic enrichment, Rotem Industries Ltd., Israel) with 16 MeV protons. ^{18}F-Separation cartridges (PS-HCO_3) were obtained from Macherey-Nagel GmbH (Germany). Reversed-phase C-18 Sep-Pak extraction cartridges were obtained from Waters Corporation (USA) and pre-conditioned with ethanol and water before use. Sodium sulfate cartridges were obtained from Varian, Inc. (USA) and used without any conditioning.

Radioactivity measurements were carried out with a CRC-15PET dose calibrator (Capintec Inc., USA), which was calibrated daily using Cs-137 and Co-57 sources (Isotope Products Laboratories, USA). Semi-preparative high-performance liquid chromatography (HPLC) separations were performed using a Dionex 680 pump with KNAUER UV detector K-2001 (KNAUER, Germany) for purification of [^{18}F]NPE and a Dionex Ultimate 3000 chromatography system with a UVD 340U absorbance detector (Dionex Corporation, USA) for purification of crude [^{18}F]FPP(RGD)$_2$. Analytical HPLC was performed using a Lab Alliance system (Lab Alliance (LA), USA) equipped with a LA Series III HPLC pump (1 mL/min), LA Model 500 UV detector (214 nm), Carroll & Ramsey Associates Model 105S radioactivity detector (CsI coupled to a PIN-diode,Carroll & Ramsey Associates, USA) and an SRI Instruments Model 202 four-channel serial port chromatography data system using PeakSimple software (SRI Instruments, USA). Isolation of [^{18}F]NPE was performed by using a Vydac column (218TP510; C-18, 5 μm, 250×10 mm, Grace, USA) with the flow rate at 5 mL/min. The gradient program started from 95% solvent A (0.1% trifluoroacetic acid (TFA) in water): 5% solvent B (0.1% TFA in acetonitrile (MeCN)) for the first 2 min and then ramped to 35% solvent A : 65% solvent B at 32 min. Purification of [^{18}F]FPP(RGD)$_2$ was performed on a Phenomenex column (Gemini, 5 μ, C18, 250×10 mm, Phenomenex, Inc., USA) with the flow rate at 7.5 mL/min. The mobile phase started from 90% solvent A: 10% solvent B (0–2 min) and then ramped to 86.5% solvent A : 13.5% solvent B at 20 min. This composition was kept at this percentage for an additional 5 min, then again gradually changed to 70% solvent A: 30% solvent B in 20 min. The final [^{18}F]FPP(RGD)$_2$ was analyzed using a Vydac column (218TP54, C-18, 5 μm, 250×4.6 mm, W.R. Grace & Co., USA) with an isocratic mobile phase (82.5% solvent A : 17.5% solvent B) at 1 mL/min.

Proton NMR was obtained with a Varian Mercury 400 MHz spectrometer (Varian, Inc., USA) using tetramethylsilane as an internal standard for the ^{1}H-NMR. Samples were also analyzed (Vincent Coates Foundation Mass Spectrometry Laboratory, Stanford University, CA, USA) using the electrospray technique in positive and negative modes with a Waters Micromass® ZQ™ single quadruple mass spectrometer (Waters Corporation, USA).

Automated Preparation of [^{18}F]FPP(RGD)$_2$

[^{18}F]NPE production was first performed in GE TRACERlab FX$_{FN}$ module within a lead-shielded hot cell (Comecer Spa, Italy). [^{18}F] Fluoride (14.8–44.4 GBq/0.4–1.2 Ci) in [^{18}O]water was transferred to the GE TRACERlab FX$_{FN}$ radiosynthesis module and passed through a PS-HCO$_3$ cartridge under vacuum. Trapped [^{18}F]fluoride ions were then eluted to the reactor with a solution containing K_2CO_3 (3.5 mg in 0.1 mL of sterile water), MeCN (0.9 mL) and 15 mg of Kryptofix 222 (4,7,13,16,21,24-hexaoxa-1,10-diazabicyclo [8.8.8] hexacosan). The solution was then evaporated at 65°C under helium flow and vacuum, followed by heating at 88°C under vacuum only. Methyl 2-bromopropionate (5 mg) in MeCN (1 mL) was added to the dried K[^{18}F]F-Kryptofix-222 complex and allowed to react at 110°C for 10 min. After cooling the reactor down to 40°C, a hydrolysis step was performed by adding 0.1 N potassium hydroxide (KOH) (0.5 mL) into the reactor and heating the alkaline mixture at 90°C for 10 min. A second azeotropic drying step was carried out with MeCN (2 mL) to remove the residual water. Once the hydrolyzed material was obtained, a solution of *bis*(4-nitrophenyl) carbonate in MeCN (2 mL and 20 mg/mL) was added to the residue and the mixture was heated at 90°C for 20 min. Upon completion of heating, the reaction mixture was diluted with sterile water (1.5 mL) and purified by the first of two semi-preparative HPLC steps for the entire [^{18}F]FPP(RGD)$_2$ radiosynthesis. The radioactive fraction corresponding to [^{18}F]NPE (Rt=22 min) was collected in a round bottom flask containing sterile water (20 mL) and then transferred to an adjacent customized

module for solid-phase extraction (SPE) using the first of two C-18 Sep-Pak cartridges for the overall production of [^{18}F]FPP (RGD)$_2$.

The coupling reaction between the [^{18}F]NPE and the cyclic peptide was carried out in an adjacent customized module. Three methods were tested to select the simplest and most efficient way to obtain anhydrous [^{18}F]NPE for the coupling reaction with PEG$_3$-c (RGDyK)$_2$. *Method 1*: The trapped [^{18}F]NPE on C-18 cartridge was eluted with MeCN (2 mL) into a vial, then the solvent was removed by rotary evaporation and the residue was resolubilized with anhydrous dimethyl sulfoxide (DMSO). *Method 2*: The trapped [^{18}F]NPE on C-18 cartridge was eluted with diethyl ether (2 mL) into a 5 mL V-vial in the customized module. The diethyl ether (Et_2O) was removed under helium stream at ambient temperature and the dried labeling agent was reconstituted with the peptide in anhydrous DMSO. *Method 3*: The last method is similar to method 2 except a sodium sulfate (Na_2SO_4) cartridge was installed just before 5 mL V-vial as an extra drying step for the eluent.

The conjugation between [^{18}F]NPE and peptide was executed using 2 mg PEG$_3$-c(RGDyK)$_2$ in anhydrous DMSO (200 μL) with DIPEA (40 μL) at 60°C for 20 min and was quenched by adding 5% acetic acid (0.7 mL). The crude [^{18}F]FPP(RGD)$_2$ product was purified with the second semi-preparative HPLC (PEG$_3$-c (RGDyK)$_2$ Rt=13 min, [^{18}F]FPP(RGD)$_2$ Rt=28 min) step. The [^{18}F]FPP(RGD)$_2$ fraction was collected, diluted with sterile water (20 mL) and sent back to TRACERlab FX_{FN} module for formulation. The diluted aqueous fraction was passed through the second C-18 Sep-Pak cartridge to trap the pure [^{18}F]FPP(RGD)$_2$. The loaded cartridge was washed with sterile water (10 mL). and [^{18}F]FPP(RGD)$_2$ was eluted from the cartridge using ethanol (United States Pharmacopeia, USP, 1 mL) and then saline (9 mL). The formulated saline mixture was sterile-filtered through a sterile Millex GS filter (0.22 μm, 4 mm) directly into a sterile product vial (30-mL size).

Quality Control (QC) Analysis of [^{18}F]FPP (RGD)$_2$

The formulated [^{18}F]FPP(RGD)$_2$ must meet all set criteria before transporting it to the clinic for human administration. A sample (1.5 mL) of [^{18}F]FPP(RGD)$_2$ was removed from the dose vial for QC analysis. Radiochemical and chemical purities were analyzed by analytical HPLC ([^{18}F]FPP(RGD)$_2$ Rt=8.9 min). The HPLC eluent was monitored for UV absorbance at 214 nm. The chemical purity of the product was >99%. A calibration curve was generated with the reference standard [^{19}F]FPP(RGD)$_2$ to allow for the determination of total carrier mass and specific radioactivity for the final batch. Based on the injection dose (555 MBq or 15 mCi) and specific radioactivity criteria (>3.7 GBq/μmol or 100 mCi/μmol), the upper mass limit of the total carrier ([^{19}F]FPP(RGD)$_2$) that can be present in the final administered dose was calculated to be 240 μg. Analysis for residual organic solvents was carried out using an Agilent 6850 GC (Agilent Technologies Inc., USA) with a capillary column (length, 30 m; ID, 0.320 mm; *df*, 0.25 μm; Agilent Technologies Inc., USA). Apyrogenicity (Charles River Laboratories Inc., USA) tests were performed in-house to ensure that doses of [^{18}F]FPP(RGD)$_2$ contained <1.25 endotoxin units per mL. ColorpHast® pH indicator strips (EMD Chemicals Inc, USA) were used to determine pH of the final product. A homemade “Bubble-Point Tester” was assembled to test the integrity of the sterile filter (> 45 psi) that was used to sterilize the final formulated [^{18}F]FPP (RGD)$_2$. The sterility tests were also performed in-house by the MIPS Radiochemistry Facility.

Mouse Studies with Clinical-Grade [^{18}F]FPP (RGD)$_2$

All animal procedures were performed according to a protocol approved by the Stanford University Administrative Panel on Laboratory Animal Care (APLAC). PET scans and image analysis were performed on female athymic nude mice (n=3, 12–14 weeks) using a microPET R4 rodent model scanner (Siemens Medical Solutions, USA). Before injection,

the tail vein was dilated by application of alcohol, heat pads or a heating lamp. Then, approximately 3.7 MBq (100 μCi) of [^{18}F]FPP(RGD)$_2$ (50–150 μL) was injected through the tail vein into the circulation of the mice under isoflurane anesthesia (1–3%). After 120 min post-injection, the animals were placed in the microPET scanner and a 3-min static whole body image was obtained. For the microPET image analyses, regions of interest (ROIs, AMIDE.exe.0.9.1) were drawn over the normal tissue and major organs on decay-corrected whole body coronal images. The radioactivity concentration (accumulation) was obtained from the mean value within the multiple ROIs and then converted to percent injected dose/g (%ID/g) or%ID (SUV).

Human Study with Clinical-Grade [^{18}F]FPP (RGD)$_2$

The radiochemistry protocol for making clinical-grade [^{18}F]FPP (RGD)$_2$ was submitted and approved as an exploratory Investigational New Drug (eIND) application by the Food and Drug Administration (FDA). A healthy volunteer (40 year-old female) was recruited and a written informed consent was obtained via an approved protocol from the Stanford University (IRB). On the day of the scan, no specific patient preparation was requested (*i.e.*, fasting and hydration). The volunteer's vital signs (heart rate, pulse oximetry, body temperature, and blood pressure) were monitored at a regular interval throughout the duration of imaging, up to 3 h post-injection using an automated machine. A 12-lead electrocardiogram (ECG) was also obtained at the same frequency and duration. Blood was obtained just prior to tracer injection for labs, as well as throughout the imaging period for time activity curve calculations. On days 1 and 7 after injection, additional vitals and blood samples were obtained to ensure stability of these parameters. Any unusual or adverse patient symptoms were also recorded on the day of imaging as well as during follow-up.

[^{18}F]FPP(RGD)$_2$ (518 MBq/14 mCi in 6 mL) was injected intravenously into a healthy human volunteer. The subject was scanned on a GE Discovery LS PET/CT scanner (GE Medical Systems, USA) in 2D mode. The volunteer had a total of 4 PET scans and 1 PET/CT scans acquired after tracer injection. The PET only scans were acquired 30, 120, and 180 min post-injection, using six bed positions (whole body scans from the skull base to the mid-thigh), 3-min emission scans, and 1-min transmission scans with a germanium rod source for attenuation correction. The PET/CT scan was acquired 1 h post-injection using a total of 11 bed positions (total body scan from the vertex to the toes) and 3-min emission scans. In this case, the CT transmission data were used for attenuation correction and anatomical localization of the PET information. The images were reconstructed using an ordered subset expectation maximization algorithm and reviewed in the axial, coronal, and sagittal planes. All reconstructions and image analysis used Xeleris software, version X (GE Healthcare Systems, USA).

Results and Discussion

Radiochemistry

All radiochemical yields (RCYs) and specific radioactivities were decay-corrected to end of bombardment as indicated and reported as means ± SD.

The multi-step radiosynthesis of [^{18}F]FPP(RGD)$_2$ (Fig. 1) was performed in a modified automated apparatus that consisted a modified commercial radiosynthesis module (TRACERlab FX$_{FN}$, GE Medical Systems) and a custommade module (Fig. 2). After a total synthesis time of 170 min, [^{18}F]FPP(RGD)$_2$ was afforded with consistent RCYs (16.9±2.7%; n=8) and specific radioactivity of 114±72 GBq/μmol (3.08±1.95 Ci/μmol, n=8). The actual amount of carrier mass measured in the final formulated dose (n=8) was 103±83 μg, which is beneath the upper mass limit of the total carrier ([^{19}F]FPP(RGD)$_2$) that can be present in the final administered dose (240 μg). Radiochemical and chemical purities

exceeded 99% via QC HPLC analysis. All other QC criteria were met in accordance with USP Chapter 823 [16].

^{18}F-Labeled target-specific peptides are generally synthesized by using an ^{18}F-prosthetic group (synthon) that will form stable chemical bonds on the peptides. A large number of ^{18}F-synthons have been developed for synthesizing the ^{18}F-radiolabeled peptides. In our previous preclinical studies [15], both *N*-succinimidyl-4-[^{18}F]fluorobenzoate ([^{18}F]SFB) and [^{18}F]NPE were synthesized for coupling with RGD-peptide. The impurity resulting from the decomposed [^{18}F] SFB lowered the RCY in the RGD-peptide coupling step, and it also adversely affected the quality of final product. However, pure [^{18}F]NPE could be obtained reproducibly via a one-pot synthesis that afforded consistent radiochemical yields which is ideal for automation. In addition, rodent PET studies with [^{18}F]SFB labeled RGD-peptide showed lower tumor to background when compared with those using the [^{18}F]NPE labeled RGD-peptide [15]. Therefore, [^{18}F]NPE was chosen as a synthon to conjugate with dimeric RGD-peptide as this tracer began its translation for use in the clinic. According to the literature [17], [^{18}F]NPE can be produced manually from methyl 2-bromopropionate via nucleophilic fluorination, hydrolysis and esterification. This simple radiochemistry was transferred to a TRACERlab FX_{FN} and pure [^{18}F]NPE was obtained by a one-pot synthesis after the first semi-preparative HPLC purification (RCY=34±12%, $n=11$) was performed. The collected HPLC fraction was subsequently trapped onto the first C-18 cartridge. [^{18}F]NPE was eluted from the loaded C-18 cartridge with MeCN to an external flask and the solvent was removed by rotary evaporation (*Method 1*). Due to the small amount of water still present in the solvent, the highly volatile 2-[^{18}F]fluoropropionic acid (bp = 66–67°C at 30 mmHg) was generated by hydrolysis of [^{18}F]NPE during the evaporation process [18]. Prior to the coupling reaction, only 8% [^{18}F]NPE was recovered based on the original amount of [^{18}F]NPE trapped on the C-18 cartridge. Although high RCY (56±25%; n=5) for the coupling-reaction step was obtained, this method still led to low overall yield of [^{18}F]FPP(RGD)$_2$.

In retrospect, the use of a rotary evaporator with our module setup still posed a challenge for the automation of the radiosynthesis. As a result, MeCN was replaced with Et_2O for eluting the first C-18 cartridge (*Method 2*) so by simply using a helium stream to remove the volatile Et_2O, this favorable change would allow for the removal of the rotary evaporation step. Since Et_2O is not generally recommended for use in the TRACERlab module, the [^{18}F]NPE SPE purification and subsequent drying steps were implemented into our customized module. Although there was almost no radioactivity loss during the transferring and drying steps of the [^{18}F]NPE preparation, low and unreliable coupling yields were still observed (30±35%; n=3).

It was suspected that residual moisture could be responsible for the hydrolysis of the labeling agent that would result in lower yields for the coupling step. In order to ensure that the Et_2O eluent was dried prior to the evaporation step, an extra Na_2SO_4 cartridge was inserted after the first C-18 Sep-Pak (*Method 3*). This extra precaution removed the trace amount of water during the elution of [^{18}F]NPE from the C-18 cartridge and it became evident that this important step was critical for achieving higher reproducible RCYs for final formulated [^{18}F]FPP(RGD)$_2$ (Table 1).

Since clinical utilization requires stricter quality control (*i.e.*, higher purity of the final product) for the radiotracer when compared with criteria set for preclinical studies, more attention is especially applied to the purification process. Small impurities were observed to be present in the formulated batch when a Vydac 218TP54 C-18 column was originally used in the radiotracer production for preclinical studies. Although these minor impurities did not seem to significantly impact our previous animal studies, these impurities needed to be

removed from the formulated batch before the radiotracer could be administered in human. Thus, a different HPLC column, Phenomenex Gemini C-18, was tested to purify the crude [^{18}F]FPP(RGD)$_2$ mixture and it fortunately provided the clinical-grade tracer in acceptable chemical and radiochemical purities.

Clinical-grade [^{18}F]FPP(RGD)$_2$ was used for the PET imaging with normal mice and a healthy human subject. Tracer uptake was represented as %ID/g (mouse, Fig. 3) or standardized uptake values (SUV; human, Table 2) as indicated.

In normal mouse studies (n=3) using clinical-grade [^{18}F] FPP(RGD)$_2$, the tracer uptake in murine kidney, bladder, liver, and muscle were determined as %ID/g (1.3±0.2, 8.7±1.3, 0.35±0.04, and 0.11±0.02) or %ID (30.4±4.7, 203.6±30.4, 8.2±0.9, and 2.6±0.5) respectively at 120 min post-injection. Selected coronal images at 120 min post-injection of clinical-grade [^{18}F]FPP(RGD)$_2$ are shown in Fig. 3. As expected, the results obtained using the higher purity tracer was reasonably consistent to our previously reported findings in mice [15].

No adverse events were monitored in the first human subject during the pilot volunteer study. As required by the FDA, a full assessment including blood pressure, ECG, and blood count were performed for acute toxicity assessment. Initial radioactivity uptake in the lung, liver, and muscle eventually cleared but high uptake was observed in the kidneys and bladder (1.3 and 8.7%ID/g or 10.1 and 32.5% ID, respectively). For the healthy human study, the images (Fig. 4) and SUV (Table 2) show stable uptake primarily in the spleen 9 liver. The radiopharmaceutical cleared through the kidneys and bladder. Lower levels of radioactivity uptake were also seen in the bowel, thyroid gland, and ventricles of the brain. [^{18}F]FPP(RGD)$_2$ was otherwise absent in the head, neck, thorax, and extremities.

Some important features for any radiotracer are (1) rapid tracer entry into and clearance from specific tissue in a time frame compatible with the radioisotope used; and (2) high specific binding to target(s) of interest with relatively low tracer binding to non-specific targets. A successful tracer should yield a high tumor to background ratio and therefore a relatively low background signal after tracer clearance is ideal. Although the current study did not yet assess the desired high tracer uptake in tumor, it is just as important to show whether the tracer cleared tissues in the time frame consistent with the half-life of fluorine-18 radioisotope, which this study has now demonstrated. The relatively low background in specific tissues such as the lungs and breast may then allow eventual success of this tracer for detecting tumors present in those locations. In addition, a brain tumor with a broken blood–brain-barrier may also allow for brain tumor/metastasis imaging. Thus, these PET imaging results with [^{18}F]FPP(RGD)$_2$ in human are quite encouraging for future clinical applications specifically for early tumor detection, staging of disease and monitoring response to therapy. Additional studies with [^{18}F]FPP(RGD)$_2$ in human volunteer subjects are already underway [19].

Conclusions

A reliable, routine and automated radiosynthesis of a new clinical-grade ^{18}F-RGD-peptide tracer ([^{18}F] FPP(RGD)$_2$) was successfully made using a modified and commercially available automated module. [^{18}F] FPP (RGD)$_2$ was administered and evaluated in the first human subject. Initial biodistribution results show the radioligand clearing through the renal system with moderate accumulation in the liver, spleen, and gut, but essentially absent background activity elsewhere. Thus, [^{18}F] FPP(RGD)$_2$ is a promising tracer with desirable pharmacokinetic properties (*e.g.*, tracer clearance from tissues to provide low background signal within a time frame compatible with the half-life of fluorine-18) for clinical

noninvasive PET imaging of $\alpha_v\beta_3$ expression. More human imaging studies, for determining the uptake of clinical-grade $FPP(RGD)_2$ in various tumor types, are currently in progress.

Acknowledgments

This research was financially supported by an NCI ICMIC P50 CA114747 Grant (SSG) and the Doris Duke foundation (SSG). We are also grateful to GE Medical Systems and Dr. David Dick for their technical support.

References

1. Tonini T, Rossi F, Claudio PP. Molecular basis of angiogenesis and cancer. Oncogene. 2003; 22:6549–6556. [PubMed: 14528279]
2. Tucker GC. Alpha v integrin inhibitors and cancer therapy. Curr Opin Investig Drugs. 2003; 4:722–731.
3. Haubner R, Decristoforo C. Radiolabelled RGD peptides and peptidomimetics for tumour targeting. Front Biosci. 2009; 14:872–886. [PubMed: 19273105]
4. Liu S. Radiolabeled cyclic RGD peptides as integrin $\alpha_v\beta_3$-targeted radiotracers: maximizing binding affinity via bivalency. Bioconjug Chem. 2009; 20(12):2199–2213. [PubMed: 19719118]
5. Decristoforo C, Hernandez GI, Carlsen J, et al. ^{68}Ga- and ^{111}In-labelled DOTA-RGD peptides for imaging of $\alpha_v\beta_3$ integrin expression. Eur J Nucl Med Mol Imaging. 2008; 35:1507–1515. [PubMed: 18369617]
6. Haubner R, Kuhnast B, Mang C, et al. [^{18}F]Galacto-RGD: synthesis, radiolabeling, metabolic stability, and radiation dose estimates. Bioconjug Chem. 2004; 15:61–69.
7. Glaser M, Morrison M, Solbakken M, et al. Radiosynthesis and biodistribution of cyclic RGD peptides conjugated with novel ^{18}F-fluorinated aldehyde-containing prosthetic groups. Bioconjug Chem. 2008; 19(4):951–957. [PubMed: 18341272]
8. Haubner R, Weber WA, Beer JA, et al. Noninvasive visualization of the activated $\alpha_v\beta_3$ integrin in cancer patients by positron emission tomography and [^{18}F]Galacto-RGD. PLoS Med. 2005; 2(3):e70. [PubMed: 15783258]
9. Kenny LM, Coombes RC, Oulie I, et al. Phase I trial of the positron-emitting Arg-Gly-Asp (RGD) peptide radioligand ^{18}F-AH111585 in breast cancer patients. J Nucl Med. 2008; 49:879–886. [PubMed: 18483090]
10. Li Z, Cai W, Cao Q, et al. ^{64}Cu-labeled tetrameric and octameric RGD peptides for small-animal PET of tumor $\alpha_v\beta_3$ integrin expression. J Nucl Med. 2007; 48:1162–1171. [PubMed: 17574975]
11. Wu Y, Zhang X, Xiong Z, et al. microPET imaging of glioma integrin $\alpha_v\beta_3$ expression using ^{64}Cu-labeled tetrameric RGD peptide. J Nucl Med. 2005; 46:1707–1718. [PubMed: 16204722]
12. Li ZB, Chen K, Chen X. ^{68}Ga-labeled multimeric RGD peptides for microPET imaging of integrin $\alpha_v\beta_3$ expression. Eur J Nucl Med Mol Imaging. 2008; 35:1100–1108. [PubMed: 18204838]
13. Wu Y, Cai W, Chen X. Near-infrared fluorescence imaging of tumor integrin $\alpha_v\beta_3$ expression with Cy7-labeled RGD multimers. Mol Imaging Biol. 2006; 8:226–236. [PubMed: 16791749]
14. Liu Z, Liu S, Wang F, Liu S, Chen X. Noninvasive imaging of tumor integrin expression using ^{18}F-labeled RGD dimer peptide with PEG_4 linkers. Eur J Nucl Med Mol Imaging. 2009; 36:1296–1307. [PubMed: 19296102]
15. Liu S, Liu Z, Chen K, et al. ^{18}F-Labeled galacto and PEGylated RGD dimers for PET imaging of $\alpha_v\beta_3$ integrin expression. Mol Imaging Biol. 2010; 12(5):530–538. [PubMed: 19949981]
16. United States Pharmacopeia. Chapter 823. USP 32 - NF 27. Radiopharmaceuticals for positron emission tomography compounding. 2009; 1:365–369.
17. Guhlke S, Coenen HH, Stocklin G. Fluoroacylation agents based on small n.c.a. [^{18}F]fluorocarboxylic acids. Appl Radiat Isot. 1994; 45:715–727.
18. Pillarsetty N, Punzalan B, Larson SM. 2-[^{18}F]-Fluoropropionic acid as a PET imaging agent for prostate cancer. J Nucl Med. 2009; 50:1709–1714. [PubMed: 19759108]

19. Mittra E, Goris ML, Iagaru AH, et al. First in man pharmacokinetic and dosimetry studies of [^{18}F]FPPRGD$_2$: A novel PET radiopharmaceutical for imaging $\alpha_v\beta_3$ integrin levels. Radiology. 2011 (in press).

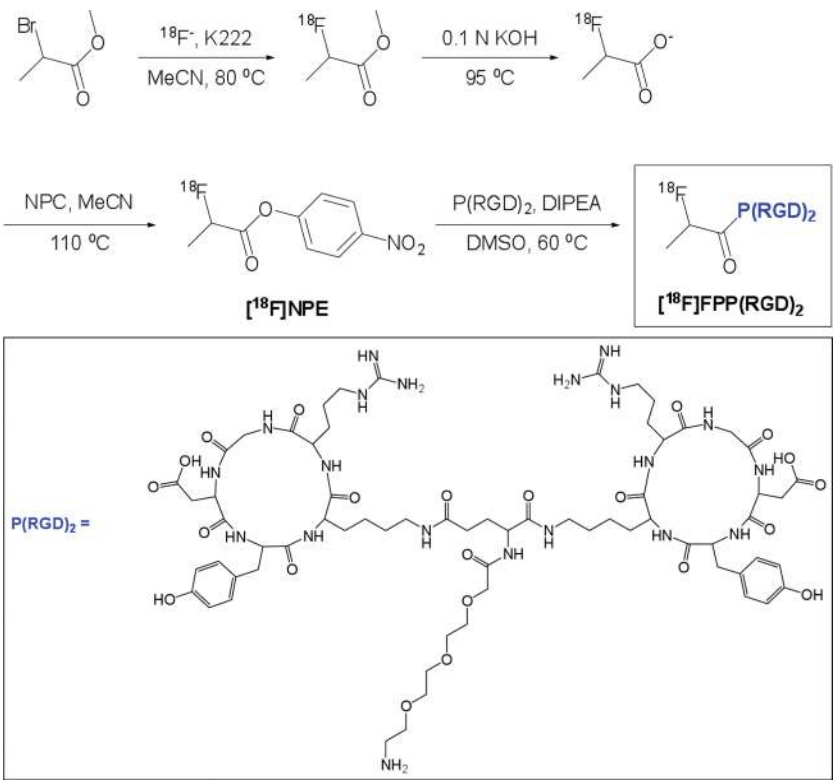

Fig. 1.
The multi-step radiosynthesis of [^{18}F]FPP(RGD)$_2$.

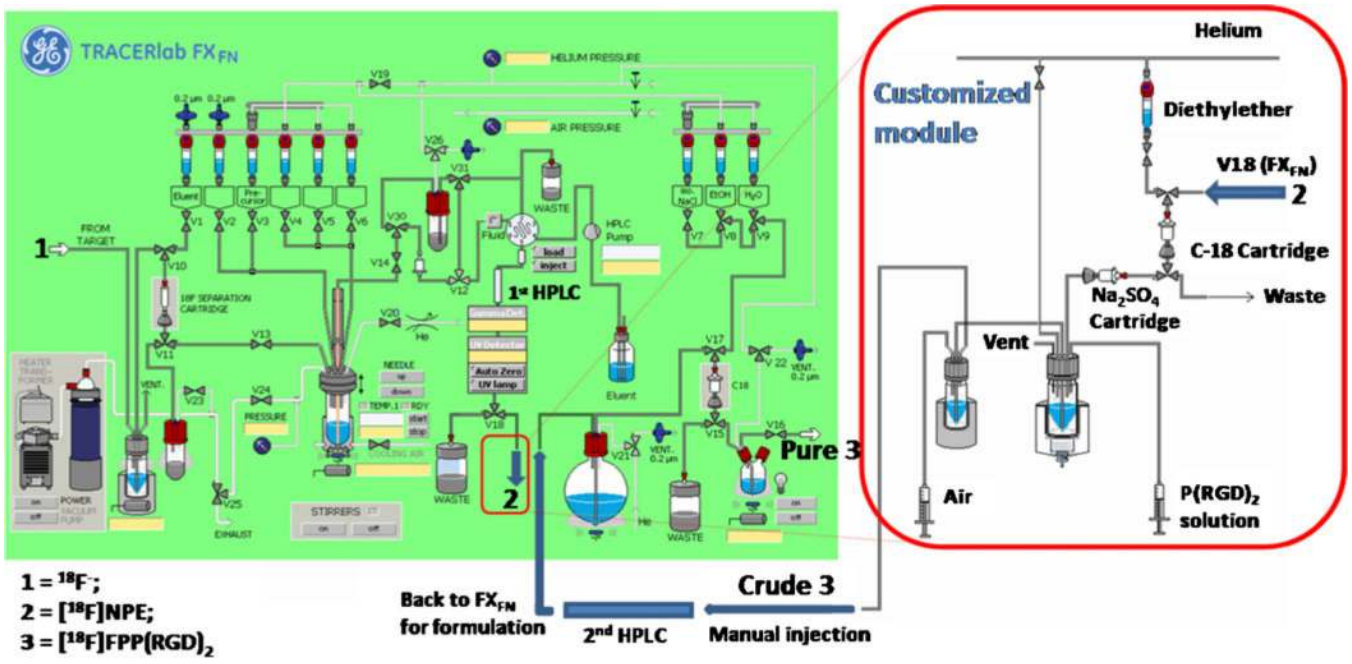

Fig. 2.

Schematic illustration of modified GE TRACERlab FXFN and customized modules (Note: GE module, customized module and 1st purification (1st HPLC) are placed in a hot cell; 2nd purification (2nd HPLC) is located outside of hot cell and shielded with lead bricks).

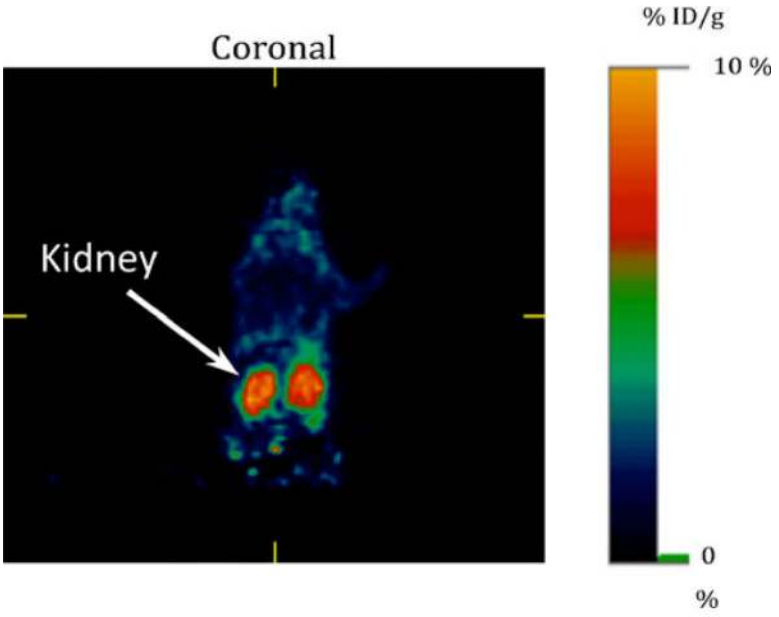

Fig. 3.
Clinical-grade [^{18}F]FPP(RGD)$_2$ injected via tail vein into a normal nude mouse and imaged 120 min post-injection (a 3D project image presented in supplement).

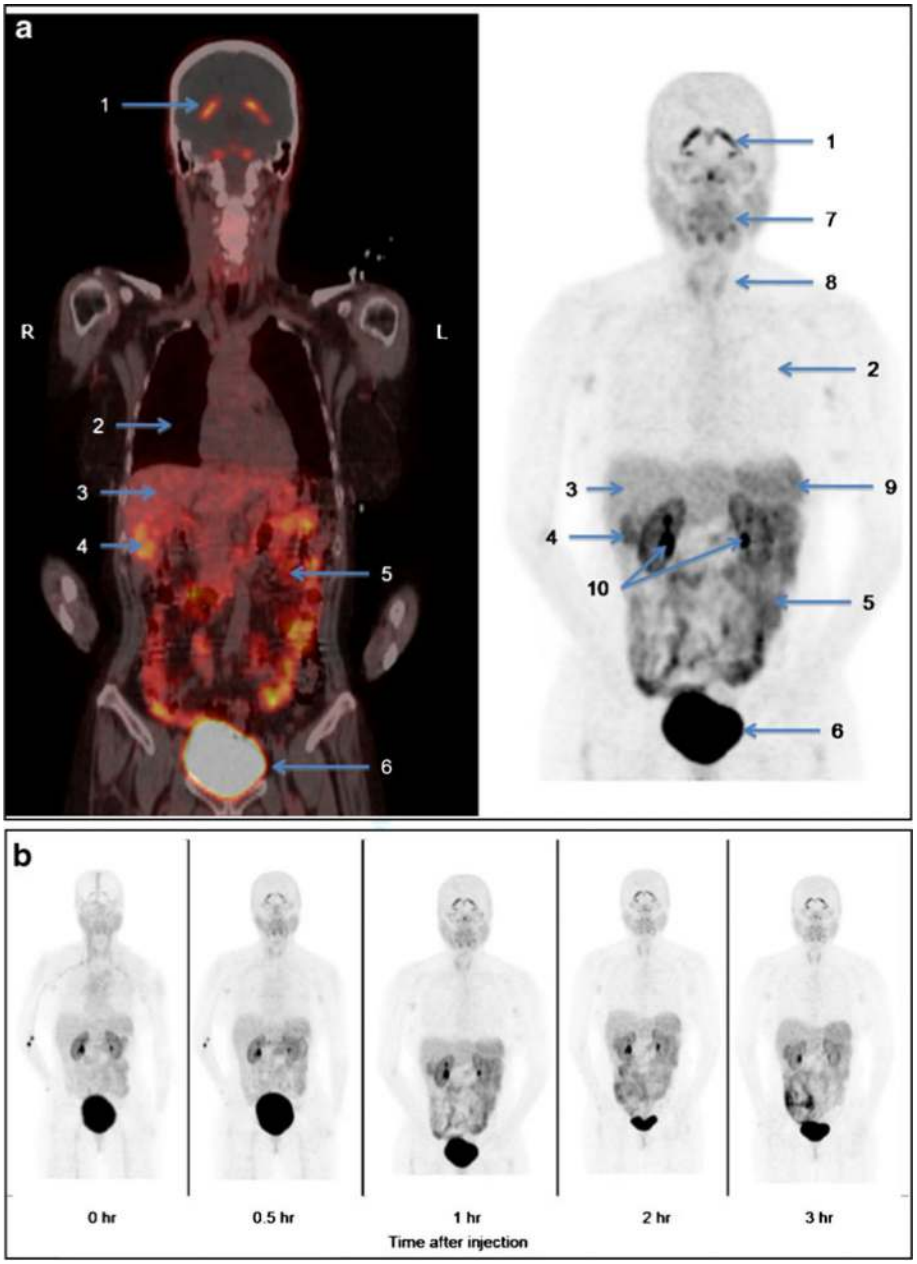

Fig. 4.

Clinical-grade [^{18}F]FPP(RGD)$_2$ (518 MBq/14 mCi) injected intravenously to a healthy human volunteer. Images include a coronal fusion PET/CT image (**a**, *left side*) and maximum intensity projection (MIP) image (**a**, *right side*) as well as serial MIP images (**b**). **a** was obtained 1-h post-injection and has the major organs of uptake labeled as follows: *1*, brain ventricles; *2*, lung; *3*, liver; *4*, gall bladder; *5*, bowel; *6*, urinary bladder; *7*, salivary glands/oropharynx; *8*, thyroid glands; *9*, spleen; and *10*, kidneys. The renal and hepatobiliary clearance routes of [^{18}F]FPP(RGD)$_2$ are evident. Above the diaphragm, there is only very limited uptake. The combined image in (**b**) shows the temporal stability of [^{18}F]FPP(RGD)$_2$ at five time-points post-injection.

Table 1

Summary of the three methods tested to select the simplest and most efficient way to obtain anhydrous [^{18}F]NPE for the coupling reaction with PEG_3-c(RGDyK)$_2$

	Method 1	**Method 2**	**Method 3**
Eluent for C18	MeCN	Et_2O	Et_2O
Removel of eluent	Rotary evaporation	Helium gas stream	Helium gas stream
Coupling yield %[a]	56±25 (*n*=5)	30±35 (*n*=3)	79.3±8.5 (*n*=9)
[^{18}F]NPE recovery %[b]	8±3 (*n*=3)	100 (*n*=3)	91±2.6 (*n*=9)
Automation	–	+	+

[a]Coupling yield is related to HPLC purification of crude [^{18}F]FPP(RGD)2: decay-corrected to end of bombardment

[b][^{18}F]NPE %=([^{18}F]NPE available for coupling reaction/[^{18}F]NPE trapped on C-18)×100%; decay-corrected to end of bombardment

Table 2

Average percent injected dose [^{18}F]FPP(RGD)$_2$ per gram (%ID/g) and standardized uptake values (SUV) normalized to weight (g/ml) for various human organs

	Time (hours)			
	0.5	**1**	**2**	**3**
Body area (% ID/g)				
Whole body	0.00455	0.00149	0.00080	0.00051
Brain ventricles	0.00349	0.00265	0.00118	0.00066
Salivary glands	0.00496	0.00180	0.00126	0.00081
Kidneys	0.01268	0.00573	0.00270	0.00151
Urinary bladder	0.04505	0.01482	0.00560	0.00371
Intestines	0.00473	0.00285	0.00208	0.00113
Liver	0.00499	0.00239	0.00169	0.00140
Spleen	0.00752	0.00484	0.00167	0.00140
Thyroid glands	0.00499	0.00258	0.00132	0.00066
Residual	0.00122	0.00045	0.00016	0.00012
SUV (g/mL)				
Brain ventricles	1.1	6.6	6.3	7.6
Kidneys	5.9	13.7	16.7	10.3
Urinary bladder	5.9	17.8	26.4	24.1
Intestines	1.5	15	6.3	9.3
Liver	2.6	2.8	4.1	5
Spleen	1.6	4.8	4.1	4.2
Thyroid glands	1.3	2.7	2.4	2.4